O. B. ISAEVA
Institute of Radio-Engineering and Electronics of RAS
Zelenaya 38, Saratov, 410019, Russia

S. P. KUZNETSOV
Institute of Radio-Engineering and Electronics of RAS
Zelenaya 38, Saratov, 410019, Russia

ON SCALING PROPERTIES OF TWO-DIMENSIONAL MAPS NEAR THE ACCUMULATION POINT OF THE PERIOD-TRIPLING CASCADE

Received September 19, 2000
DOI: 10.1070/RD2000v005n04ABEH000159

We analyse dynamics generated by quadratic complex map at the accumulation point of the period-tripling cascade (see Golberg, Sinai, and Khanin, Usp. Mat. Nauk. V. 38, No 1, 1983, 159; Cvitanović and Myrheim, Phys. Lett. A94, No 8, 1983, 329). It is shown that in general this kind of the universal behavior does not survive the translation two-dimensional real maps violating the Cauchy – Riemann equations. In the extended parameter space of the two-dimensional maps the scaling properties are determined by two complex universal constants. One of them corresponds to perturbations retaining the map in the complex-analytic class and equals $\delta_1 \cong 4.6002 - 8.9812i$ in accordance with the mentioned works. The second constant $\delta_2 \cong 2.5872 + 1.8067i$ is responsible for violation of the analyticity. Graphical illustrations of scaling properties associated with both these constants are presented. We conclude that in the extended parameter space of the two-dimensional maps the period tripling universal behavior appears as a phenomenon of codimension 4.

The paper is dedicated to the 150-th anniversary of Sofia Kovalevskaya

1. Introduction

One of the most popular illustrations in the nonlinear science is a picture of the Mandelbrot set [1, 2] (Fig. 1). This is the set of points on the plane of complex parameter λ, at which the iterations of the complex quadratic map

$$z' = \lambda - z^2, \quad \lambda, z \in \mathbb{C} \tag{1.1}$$

starting from the critical point $z = 0$ never go to infinity. (Here the prime marks the dynamical variable relating to the next iteration, i. e. to the next moment of the discrete time.)

The Mandelbrot set has subtle and complicated structure, which is a subject of numerous researches. Objects analogous to the Mandelbrot set are also presented in parameter spaces of other complex analytic iterative maps [2, 3]. It is worth stressing that instead of the one-dimensional complex analytic maps we can consider an equivalent class of two-dimensional real maps satisfying the Cauchy – Riemann equations.

It is used to regard the Mandelbrot set as a classic example of fractal, which suggests a sort of self-similarity, or scaling. In fact, as shown by Milnor [4], the "hairiness" intrinsic to the Mandelbrot set does not reproduce itself on deep levels of resolution of the small-scale structure, but becomes more expressed there. So, the property of self-similarity should be related rather to a definite subset called "the Mandelbrot cactus" [4, 5]. The cactus includes the domain of existence of a stable fixed point and domains of stable orbits of different periods, which originate from the fixed point via all possible bifurcation sequences (see the gray colored part of the picture in Fig. 1).

Mathematics Subject Classification 58F36

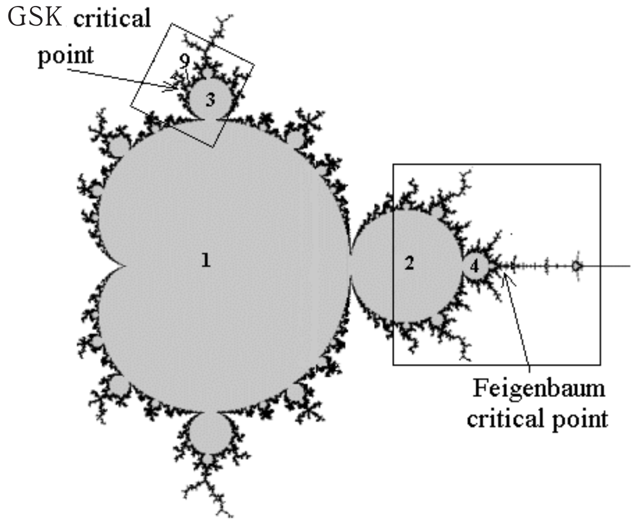

Fig. 1. Mandelbrot set for complex analytic quadratic map (1.1). The gray colored areas form the Mandelbrot cactus. Periods associated with the leaves of the cactus are designated by the respective numbers. Two frames mark areas of scaling near the points of period-doubling and period-tripling

One particular manifestation of scaling on the cactus is associated with the Feigenbaum period-doubling cascade. The leaves of the cactus are placed along the real axis and corresponded to stable attractive orbits of period 2, 4, 8, ... , 2^k, ... They reproduce each other more and more precisely under subsequent magnification by the universal scaling factor defined by the real constant $\delta_F \cong 4.6692$. The limit point of the period-doubling accumulation is placed on the real axis at $\lambda^{\mathrm{dbl}} = 1.401155189\ldots$. The scaling properties intrinsic to the neighborhood of this point follow from the renormalization group (RG) analysis developed by Feigenbaum [6, 7]. Behavior of the function representing the solution of the basic equation of the theory, the Feigenbaum – Cvitanović equation, in complex domain was discussed e. g. in works of Nauenberg [10] and Wells and Overill [11].

Beside the Feigenbaum point one can find on the complex parameter plane many other points, at which the Mandelbrot cactus displays properties of self-similarity. In particular, we can select a path on the complex plane λ through across the sequence of leaves corresponding to periods 3, 9, 27, ... , 3^k, ..., and arrive at the period-tripling accumulation point

$$\lambda_c^{\mathrm{tripl}} = 0.0236411685377 + 0.7836606508052i. \tag{1.2}$$

This point was first discovered by Golberg, Sinai, and Khanin [12], and then, independently, by Cvitanović and Myrheim [5, 13]. For shortness, we will refer to it as the GSK *critical point*. As in the case of period-doubling, dynamics at the GSK point allows the RG analysis. In particular, it leads to a conclusion on the property of similarity for the associated leaves of the the Mandelbrot cactus. According to Refs. [12, 13, 5], the scaling factor appears to be complex and equal to $\delta_1 \cong 4.6002 - 8.9812i$[1].

It seems very interesting to discuss a possibility to observe phenomena of the complex analytic dynamics associated with the Mandelbrot set in physical systems. Recently this question was posed by Beck [14]. The author considered motion of a charged particle in a double-well potential in a time-depended magnetic field and showed that under certain assumptions, the dynamics can be described by the complex quadratic map or by other complex analytic maps.

It should be emphasized that when estimating a possibility of physical realization for any special type of dynamics we should account robustness of a phenomenon under study. In particular, one has

[1]Beside (1.2) a complex conjugate period-tripling accumulation point exists at $\lambda = \lambda_c^*$, and scaling constant for it equals δ_1^*.

to ask either various phenomena associated with dynamics of the complex analytic iterative maps will survive or not in a slightly modified map, which could violate the Cauchy–Riemann conditions.

In the original work [12] the authors claimed that the infinite period-tripling bifurcation cascade could occur typically in two-parameter families of real two-dimensional maps (see also [15]). In contrast, from studies of Peinke et al. [16], Klein [17], and from qualitative analysis of Cvitanović and Myrheim [5] it follows that in presence of a non-analytic perturbation of the map the arrangement of the parameter space is changed drastically, and, apparently, it leaves no opportunity for the universality intrinsic to the period-tripling and to the GSK point to survive. Recently Peckham and Montaldi have presented extensive bifurcation analysis of the complex quadratic map with a non-analytic term [18, 19]. However, the question what happens with the bifurcation cascades of period-tripling in presence of this term remains not clear. Apparently, this matter deserves special consideration in terms of the RG analysis. This is the main goal of the present article. Our final conclusion is that the critical behavior associated with the infinite period-tripling bifurcation cascade in real two-dimensional maps will occur typically only in families having at least four real parameters. In other words, the codimension of the phenomenon is four. On this reason its physical observation seems problematic.

In Section 2 we reproduce the contents of the RG analysis developed in Refs. [12, 13, 5] and extend it to study the RG equation fixed point in respect to a class of perturbations, which can violate the Cauchy–Riemann conditions. We find that one of the eigenvalues for the linearized RG transformation associated with a non-analytic perturbation is relevant. In Section 3 we formulate the model map appropriate for a study of dynamics in the extended parameter space. Then we explain a necessity of nonlinear variable change to define local coordinates for observation of scaling in the parameter space. (The procedure of numerical calculations used to find the desired variable change is described in the Appendix.) In Section 4 we discuss some details of the parameter space arrangement near the GSK point and present graphical illustrations of the intrinsic scaling properties associated with both relevant universal constants.

2. Renormalization group analysis

For the original model Eq. (1.1) determines the evolution operator over one iteration step. Then, for three iterations we have, obviously, $z' = f(f(f(z))) = \lambda - (\lambda - (\lambda - z^2)^2)^2$. Let us introduce the new variable, which differs from z by a constant factor α_0. We select the value of this factor to normalize the new map corresponding to the three-step evolution operator to unity at the origin. Then the result may be written as $z' = f_1(z)$, where $f_1(z) = \alpha_0 f(f(f(z/\alpha_0)))$, and $\alpha_0 = 1/f(f(f(0)))$.

Now we can take $f_1(z)$ as the initial function and apply the same procedure. The result will be the renormalized evolution operator for nine steps: $z' = f_2(z)$, where $f_2(z) = \alpha_1 f_1(f_1(f_1(z/\alpha_1)))$, $\alpha_1 = 1/f_1(f_1(f_1(0)))$. Multiple repetition of the transformation yields the recurrent functional equation in the following form:

$$f_{k+1}(z) = \alpha_k f_k(f_k(f_k(z/\alpha_k))), \qquad \alpha_k = 1/f_k(f_k(f_k(0))). \tag{2.1}$$

Here $f_k(z)$ represents the evolution operator for 3^k iterations of the original map in terms of the renormalized dynamical variable. Note that the constants of rescaling α_k, which appear at the subsequent steps of the procedure, are complex.

According to results of the previous works [12, 13, 5], at the period-tripling accumulation point the sequence of functions $f_k(z)$ converges to certain limit $g(z) = \lim\limits_{k\to\infty} f_k(z)$, where $g(z)$ is a universal function being the fixed point of the RG equation

$$g(z) = \alpha g(g(g(z/\alpha))), \quad \alpha = \lim_{k\to\infty} \alpha_k = 1/g(g(g(0))). \tag{2.2}$$

It is just a generalization of the Feigenbaum–Cvitanović equation [6, 7] for the case of period-tripling. Obviously, the function $g(z)$ has to be even, with quadratic critical point at $z = 0$, because these are

Table 1. The coefficients of polynomial expansion for the fixed-point function $g(z)$

1	$1.0 + 0.0i$
z^2	$0.054665304 - 0.749020944i$
z^4	$-0.024397241 - 0.052466461i$
z^6	$-0.002529112 - 0.001197430i$
z^8	$-0.000088081 + 0.000137556i$
z^{10}	$0.000000729 + 0.000018289i$
z^{12}	$0.000000541 + 0.000001194i$
z^{14}	$0.000000074 + 0.000000048i$

the properties of all the functions in the sequence $f_k(z)$. For numerical solution of the equation (2.2) one can approximate the function $g(z)$ by a finite Taylor series containing only even powers of z:

$$g(z) = 1 + \sum_{r=1}^{m} g_r z^{2r}. \tag{2.3}$$

Next, we can realize the RG transformation as the computer program operating with the coefficients of the polynomial expansions. Conditions of equality for terms of identical powers in the left- and right-hand parts of the equation (2.2) determine a certain set of nonlinear algebraic equations, which can be solved numerically by means of multi-dimensional Newton method. In Table 1 we present the coefficients of the polynomial expansion for the universal function, which are in good agreement with the earlier data of Refs. [12, 13]. As follows from the computations, the scaling constant is

$$\alpha = -2.09691989 + 2.35827964i. \tag{2.4}$$

To simplify further analysis it is useful to redefine the RG transformation accounting that the constant α is known now. Namely, we prefer to use now the same rescaling factor at all subsequent steps of the renormalization, assuming that it is independent on the index k and equal α. We just substitute $\alpha_k = \alpha$ into Eq. (2.1) and obtain

$$f_{k+1}(z) = \alpha f_k(f_k(f_k(z/\alpha))). \tag{2.5}$$

Obviously, the new version of the RG transformation possesses the same fixed point $g(z)$ as Eq. (2.1) has, although the normalization $g(0) = 1$ should be regarded now as an arbitrarily accepted additional condition.

Let us consider the map $z' = g(z)$, where $g(z)$ is the function associated with the fixed-point of the RG transformation. Using the data of Table 1 one can check that this map has an unstable fixed point $z = z_* \cong 0.691473 - 0.302692i$, and derivative at this point is

$$\mu_c = g'(z_*) = -0.47653180 - 1.05480868i. \tag{2.6}$$

Then, it follows from Eq. (2.2) that starting at z_*/α we obtain an orbit of period 3. The Floquet eigenvalue (or multiplier) for this cycle is the same complex number μ_c. By induction, it is easy to see that there is an infinite countable set of period-3^k cycles with the same value of the multiplier. As the mapping $z' = g(z)$ represents the asymptotic form of the evolution operators for the original map, one can conclude that the map (1.1), as any other map relating to the universality class, must have an infinite set of the unstable orbits of period 3^k at the GSK point. Asymptotic value of the multipliers is the universal constant μ_c.

Now let us consider some smooth real two-dimensional map

$$x' = \varphi(x, y), \quad y' = \psi(x, y), \tag{2.7}$$

which depends on several parameters. In terms of the complex variable this map can be expressed, in general, as a function of two arguments $z = x + iy$ and $z^* = x - iy$: $z' = F(z, z^*)$, where $F(x+iy, x-iy) = \varphi(x, y) + i\psi(x, y)$. Next, let us assume that in the parameter space there is a point, at which the map is complex analytic, i. e. the Cauchy–Riemann equations hold: $\varphi_x = \psi_y$, $\varphi_y = -\psi_x$, and the dynamics in this point is intrinsic to the period-tripling accumulation point GSK. It means that for a sufficiently large number of iterations 3^k the evolution operator in appropriate normalization is represented by the universal function $g(z)$. If we slightly change the parameters and depart from the GSK point, the behavior of the evolution operator sequence is distinct and near the fixed point some perturbation of the RG equation solution appears. In general, the perturbed solution does not satisfy the Cauchy–Riemann conditions, so the evolution operator should be written in the following form:

$$F_k(z) = g(z) + \varepsilon h_k(z, z^*). \tag{2.8}$$

Here $\varepsilon \ll 1$, and h_k is a smooth function of two arguments. Let us substitute the last expression into the RG equation (2.5) and collect the terms of the first order in ε. It yields

$$\begin{aligned} h_{k+1}(z, z^*) = \alpha[g'(g(g(z/\alpha)))g'(g(z/\alpha))h_k(z/\alpha, (z/\alpha)^*) + \\ + g'(g(g(z/\alpha)))h_k(g(z/\alpha), (g(z/\alpha))^*) + h_k(g(g(z/\alpha)), (g(g(z/\alpha)))^*)], \end{aligned} \tag{2.9}$$

where g' means the derivative of the function g. Obviously, this relation has a structure $h_{k+1} = \widehat{m}h_k$, where $\widehat{m}$ is a linear operator defined by the right-hand part of (2.9) and acting in a space of functions $h(z, z^*)$. The question of behavior of the solution for the linearized RG equation under iterations is linked with the spectrum of eigenvalues of the operator $\widehat{m}$. Those eigenvalues are relevant, which absolute value are larger than 1 because the corresponding components of the perturbation grow under subsequent iterations of the RG transformation. So, we arrive at the following eigenproblem:

$$\begin{aligned} \nu h(z, z^*) = \alpha[g'(g(g(z/\alpha)))g'(g(z/\alpha))h(z/\alpha, (z/\alpha)^*) + \\ + g'(g(g(z/\alpha)))h(g(z/\alpha), (g(z/\alpha))^*) + h(g(g(z/\alpha)), (g(g(z/\alpha)))^*)]. \end{aligned} \tag{2.10}$$

The numerical solution of the eigenproblem can be obtained by using of the polynomial representation for the function $g(z)$, which is already known, and with the help of Taylor expansion for the function $h(z, z^*)$ in powers of z and z^*. As we account a finite number of the terms in the expansions, the eigenproblem becomes a finite-dimensional one, and reduces to a search for eigenvectors and eigenvalues of a certain matrix. As the numerical calculations show, the senior eigenvalue equals

$$\delta_1 = 4.60022558 - 8.98122473i, \tag{2.11}$$

and the associated eigenfunction does not depend on the second argument z^*. In Table 2 we present the coefficients of the polynomial expansion for the eigenfunction $h^{(1)}(z)$. We can see that the function is even. The universal constant (2.11) was found in Ref. [12], where the RG equation solutions in the form $f_k(z) = g(z) + \varepsilon h_k(z)$ were considered. It is clear that the perturbation of such type retains the map in the class of mappings satisfying the Cauchy–Riemann equations.

It appears, however, that one more relevant eigenvalue exists, which is larger than unity in modulus, and is responsible for non-analytic perturbation of the fixed point of the RG equation. The associated eigenfunction contains the powers of both arguments z and z^* in the polynomial expansion. Let us turn first to an analytical derivation indicating presence of such a solution.

We have mentioned that the fixed-point function $g(z)$ is even. Hence, it follows from (2.10) that

$$\begin{aligned} \nu h(-z, -z^*) = \alpha[g'(g(g(z/\alpha)))g'(g(z/\alpha))h(-z/\alpha, -(z/\alpha)^*) + \\ + g'(g(g(z/\alpha)))h(-g(z/\alpha), -(g(z/\alpha))^*) + h(-g(g(z/\alpha)), -(g(g(z/\alpha)))^*)]. \end{aligned} \tag{2.12}$$

Table 2. The coefficients of polynomial expansion for the senior eigenfunction $h^{(1)}(z)$

1	$1.0 + 0.0i$
z^2	$0.181223377 - 0.141361034i$
z^4	$0.002303322 - 0.015962515i$
z^6	$-0.001131785 - 0.000491487i$
z^8	$-0.000151737 + 0.000053131i$
z^{10}	$-0.000010514 + 0.000009686i$
z^{12}	$-0.000000310 + 0.000001085i$
z^{14}	$0.000000033 + 0.000000100i$

Let us represent the eigenfunction as a sum of the symmetric and antisymmetric components:

$$h(z, z^*) = h^s(z, z^*) + h^a(z, z^*), \tag{2.13}$$

where

$$h^s(z, z^*) = \frac{h(z, z^*) + h(-z, -z^*)}{2}, \tag{2.14}$$

$$h^a(z, z^*) = \frac{h(z, z^*) - h(-z, -z^*)}{2}. \tag{2.15}$$

Then, subtracting (2.12) from (2.10) we have

$$\nu h^a(z, z^*) = \alpha g'(g(g(z/\alpha)))g'(g(z/\alpha))h^a(z/\alpha, (z/\alpha)^*). \tag{2.16}$$

Now let us express the function $h^a(z, z^*)$ as

$$h^a(z, z^*) = \frac{g'(z)}{z}\Phi(z, z^*), \tag{2.17}$$

where $\Phi(z, z^*)$ is a smooth function without singularity at $z \to 0$. As we have $g'(z) \propto z$, the ratio $g'(z)/z$ does not possess a singularity at $z = 0$, and our representation is reasonable. Using the relation

$$g'(g(g(z/\alpha)))g'(g(z/\alpha))g'(z/\alpha) = 1, \tag{2.18}$$

which follows from (2.2), we obtain a simple equation for the function $\Phi(z, z^*)$:

$$\nu\Phi(z, z^*) = \alpha^2\Phi((z/\alpha), (z/\alpha)^*). \tag{2.19}$$

Obviously, any product $z^M(z^*)^N$ where integers $M \geqslant 0, N > 0$ and the sum $M + N$ is odd, yields an eigenfunction, and the associated eigenvalue is $\alpha^{2-M}(\alpha^*)^{-N}$. Observe that modulus of one these numbers is larger than one. Indeed, setting $M = 0$ and $N = 1$, i. e. $\Phi = z^*$, we obtain

$$h^a(z, z^*) = \frac{g'(z)}{z}z^*, \tag{2.20}$$

and

$$\nu = \frac{\alpha^2}{\alpha^*} = \delta_2 = 2.58728651 + 1.80679396i. \tag{2.21}$$

Table 3. The coefficients of polynomial expansion for the eigenfunction $h^{(2)}(z, z^*)$ associated with the eigenvalue $\delta_2 = 2.58728651 + 1.80679396i$

	1	z^*	$(z^*)^2$	$(z^*)^4$	$(z^*)^6$	$(z^*)^8$
1	$1.0 + 0.0i$	-3.029846 $+6.351031i$	0.398114 $+0.008514i$	-0.022670 $-0.073276i$	-0.002329 $-0.003512i$	-0.000073 $-0.0002278i$
z^2	1.094504 $-1.043125i$	0.068249 $+1.082134i$	0.086111 $+0.039504i$	-0.001995 $+0.001278i$	-0.000053 $+0.000130i$	0.0000004 $+0.000006i$
z^4	-0.048082 $-0.141290i$	0.053978 $+0.057211i$	0.001900 $-0.001493i$	-0.000124 $+0.000212i$	0.0000003 $+0.000009i$	
z^6	-0.011263 $-0.005046i$	0.004950 $-0.003601i$	-0.000450 $-0.000460i$	-0.000005 $+0.000022i$		
z^8	-0.000616 $+0.000710i$	0.000280 $-0.000811i$	-0.000058 $-0.000028i$	0.0000002 $+0.000002i$		
z^{10}	-0.000002 $+0.000109i$	-0.000004 $-0.000074i$	-0.000004 $+0.0000002i$			

Table 4. Some eigenfunctions of the eigenproblem (2.10) associated with the infinitesimal variable changes

Variable change, $\Delta \ll 1$	Eigenfunction $h(z, z^*)$	Eigenvalue ν
Shift: $z \to z + \Delta$	$g'(z) - 1$	$\nu = \alpha = -2.0969 + 2.3583i$
Scale change $z \to z(1 + \Delta)$	$zg'(z) - g(z)$	$\nu = 1$
Non-analytic change $z \to z + z^* \cdot \Delta$	$z^* g'(z) - (g(z))^*$	$\nu = \alpha/\alpha^* = -0.1169 - 0.9931i$ $\lvert\nu\rvert = 1$

So, we come to the conclusion that the relevant eigenvector depending on z^* does exist. From numerical solution of the linearized RG equation based on the expansion of the function $h(z, z^*)$ in powers of z and z^*

$$h^{(2)}(z, z^*) = \sum_{i,j=0}^{n} h_{ij} z^i z^{*j} \tag{2.22}$$

we have obtain the eigenvalue

$$\delta_2 = 2.58728651 + 1.80679396i \tag{2.23}$$

and the coefficients presented in Table 3. The coefficients absent in the table are zero. As one can see, the antisymmetric part of the function $h^{(2)}(z, z^*)$ is represented by the second column of the table. It may be checked that this component coincide up to a constant factor with the analytical result (2.17), and the eigenvalue consides with (2.20).

All eigenvalues distinct from δ_1 and δ_2 are not relevant. Some of them are associated with infinitesimal variable changes (cf. [7]). Such eigenfunctions can be expressed explicitly via the fixed point function $g(z)$, see Table 4. As the numerical calculations show, the modules of all other eigenvalues are less than one.

As it follows from our analysis, the condition of realization of the universal behavior characteristic for the GSK point is a possibility to vanish coefficients of two relevant eigenvectors associated with

δ_1 and δ_2 by tuning the control parameters of the map. It yields two complex, or four real, equations on the parameters. Generically, the solution will exist if the number of variables is not less than the number of equations. So, we conclude that the universal behavior GSK may occur as generically in a space of four real parameters. In other words, this is the dynamical behavior of codimension four.

It is worth noting that in general the Cauchy–Riemann equations are not necessary for existence of the GSK point. For example, let us turn to the map studied by Gunaratne [15]

$$\begin{aligned} x' &= a + x^2 - y^2, \\ y' &= b + (2+\varepsilon)xy. \end{aligned} \tag{2.24}$$

In this particular case the non-analytic term does not contribute into the eigenvector h_2. Indeed, by means of the variable changes $z = x + yi$, $\lambda = a + ib$ and $\varepsilon = \varepsilon/4$ this map can be reduced to $z' = \lambda + z^2 + \varepsilon(z^2 - (z^*)^2)$. Here the non-analytic term has form $(z^*)^2$. Because the linear component z^* is absent, this non-analytic perturbation cannot contain the second eigenvector. It contributes into the first eigenvector, but this perturbation may be compensated by an appropriate shift of $\lambda = a + ib$. Thus, the GSK point does exist, and it agrees with the conclusion of Ref. [15]. According to our computations, for $\varepsilon = 0.2$ the critical point is located at $a \cong -0.035475$, $b \cong 0.747736$.

3. Model map and local scaling coordinates near the GSK point

Let us construct a model map appropriate for a study of dynamics in a neighbourhood of the GSK point in the extended parameter space.

If we take the complex quadratic map (1.1) then a variation of parameter λ with departure from the GSK point give rise, obviously, only to a perturbation that does not violate the analyticity; the growing contribution in the solution of the linearized RG equation is given only by the eigenfunction $h^{(1)}(z)$. As we wish to turn on a perturbation of type $h^{(2)}(z, z^*)$, it is necessary to add an appropriate non-analytic term in the map. Accounting that this eigenfunction $h^{(2)}(z, z^*)$ behaves for small $|z|$ as $h^{(2)} \propto z^*$, it is natural to add the term proportional to z^*. Thus, we come to the model map

$$z' = f(z) = \lambda - z^2 + \varepsilon z^*. \tag{3.1}$$

Up to a trivial variable change ($z \to -z$) this is the same map that the authors of Refs. [18, 19] choose for their extensive bifurcation analysis. The extended parameter space is the two-dimensional complex space $\mathscr{C}^2 : (\lambda, \varepsilon)$. Note that the map (3.1) is equivalent to a four-parameter two-dimensional real map

$$x_{n+1} = a - x_n^2 + y_n^2 + ux_n + vy_n, \qquad y_{n+1} = b - 2x_ny_n + vx_n - uy_n, \tag{3.2}$$

where we set $z = x + iy$, $\lambda = a + ib$, $\varepsilon = u + iv$.

As we have two relevant eigenfunctions $h_1(z)$ and $h_2(z, z^*)$, the sequence of the evolution operators generated by repetitive application of the RG transformation behave as

$$f_k(z, z^*) = g(z) + C_1(\lambda, \varepsilon)\delta_1^k h^{(1)}(z) + C_2(\lambda, \varepsilon)\delta_2^k h^{(2)}(z, z^*); \tag{3.3}$$

this is true in linear approximation with respect to the deviation from the fixed point $g(z)$. Here C_1 and C_2 are some complex coefficients, which vanish at the GSK point ($\lambda = \lambda_c, \varepsilon = 0$).

It would be convenient to use the coefficients C_1 and C_2 as local coordinates in parameter space. In these coordinates the scaling properties of the parameter space are very simple and evident. Indeed, if we change C_1 to C_1/δ_1 and C_2 to C_2/δ_2, then, according to (3.3), the evolution operator f_{k+1} at the new point takes the same form as the operator f_k at the old point. It means that the similar dynamical regimes, but with tripled characteristic time scale, will occur at the new point.

Unfortunately, we do not know the form of explicit expressions for $C_1(\lambda, \varepsilon)$ and $C_2(\lambda, \varepsilon)$. Hence, the coordinate system in the parameter space suitable for demonstration of scaling (*the scaling coordinates*) must be found numerically with sufficient precision.

Equation $C_1(\lambda, \varepsilon) = 0$, or, in alternative notation, $C_1(a, b; u, v) = 0$ defines some manifold M in the parameter space.

Let us rewrite the equation of the manifold M in a form

$$a = a_c + F(u, v), \qquad b = b_c + G(u, v), \tag{3.4}$$

where a_c and b_c correspond to the GSK point. The functions $F(u, v)$ and $G(u, v)$ may be represented as Taylor expansions in powers of u and v. It occurs that the terms of the third and higher order can be neglected on the following reason. As we will require, the renormalization of the complex coordinate $\varepsilon = u + iv$ by factor δ_2 has to ensure realization of similar dynamical regime. Let us assume that we miss some term of power m in the expansion of F or G. When we perform scale change $\varepsilon \to \varepsilon/\delta_2$, this term will have an order δ_2^{-mk}, and the error in the amplitude of the senior eigenvector will behave as δ_1^k/δ_2^{mk}. Accounting our concrete relation of the eigenvalues intrinsic to the GSK point we observe that it is dangerous only for $m \leqslant 2$, otherwise the error asymptotically vanishes as $k \to \infty$. Indeed, in accordance with (2.11) and (2.21) we have $|\delta_2| < |\delta_1|$ and $|\delta_2|^2 < |\delta_1|$, but $|\delta_2|^3 > |\delta_1|$. So, only the terms of the first and second order in the Taylor expansion must be evaluated accurately. So, we rewrite the original map as follows:

$$\begin{aligned} x' &= a - x^2 + y^2 + ux + vy + Au + Bv + Pu^2 + Quv + Rv^2, \\ y' &= b - 2xy + vx - uy + Cu + Dv + Su^2 + Tuv + Hv^2, \end{aligned} \tag{3.5}$$

where the capital letters designate the coefficients, which can be computed by means of the procedure described in Appendix:

$$\begin{gathered} A = -0.232750391, \quad B = 0.02699484, \quad C = -B, \quad D = A, \\ P = -0.2173, \quad Q = -0.070, \quad R = -0.3184, \\ S = 0.1533, \quad T = 0.1010, \quad H = 0.083. \end{gathered} \tag{3.6}$$

The coordinate system $(a, b; u, v)$ is appropriate for demonstration of scaling because a shift of u and v will contribute only into the second eigenvector, while a shift of a and b, as we know, contributes only into the first eigenvector[2].

4. Scaling properties of the extended parameter space in a neighborhood of the GSK point

The complete bifurcation analysis in the four-dimensional parameter space (a, b, u, v) would be complicated and tedious (see, nevertheless, Refs. [18, 19]). Here we only want to present computer illustrations for scaling properties following from the RG results of Section 2. For this aim we will consider certain two-dimensional cross-sections of the parameter space and demonstrate self-similarity of structures observed in these cross-sections.

For graphical presentation we will use the technique of "Lyapunov space", or Lyapunov charts (see [21, 22, 23] for previous applications of this method). As we have chosen the parameter space cross-section to be studied, we compute the senior Lyapunov exponent for the model map at each pixel of the two-dimensional plot, and mark this pixel by a certain gray tone. We code the negative values of Lyapunov exponent from $-\infty$ to 0 by tones from dark to light gray (it corresponds to the periodic regimes). White color represents zero Lyapunov exponent (e. g. quasiperiodicity or states

[2]See other examples of nonlinear parameter change for observation of the multi-parameter scaling in Refs. [24, 25, 26].

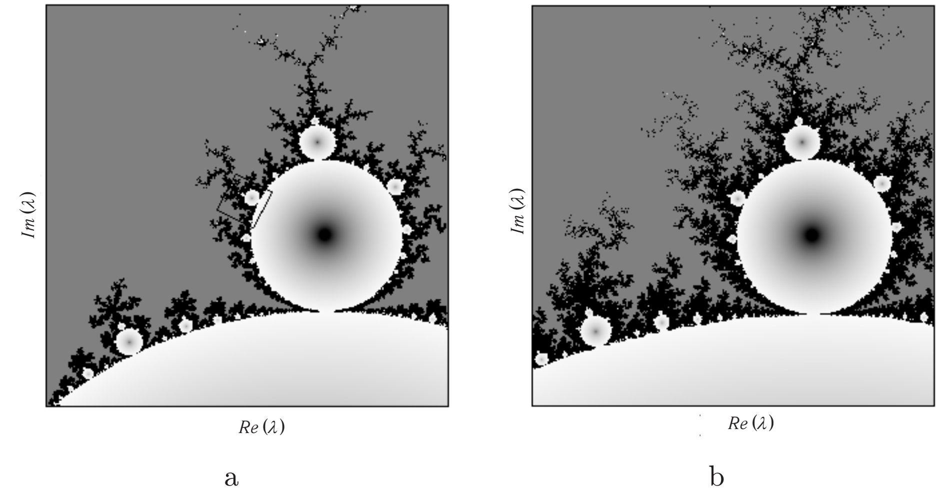

Fig. 2. Cross-section of the parameter space for the map (3.1) by a plane $u = 0$, $v = 0$. Gray tones from dark to light code values of the Lyapunov exponent from large negative to zero. White color corresponds to zero, and black corresponds to positive Lyapunov exponent. Divergence is shown by uniform coloring with one special gray tone. The GSK point is located exactly at the center of the diagrams. Fig. (b) shows a fragment of Fig. (a) inside the frame after magnification and rotation in accordance with multiplication by $\delta_1 \cong 4.6002 - 8.9812i$. The coding rule on the right plot is redefined to account the tripling of the characteristic time scales

at the onset of chaos), and black — positive Lyapunov exponent (chaos). Such a convention for the palette ensures a clear vision of the border between regular and chaotic dynamics. In some domains of the parameter space the model map manifests divergence; these areas are colored uniformly by one special gray tone.

In our computations the trajectories started each time from the point $z = 0$, and the calculations for evaluation of the Lyapunov exponent began after some sufficiently large number of iterations to exclude the transients.

Let us turn first to a properties of scaling following from results of Refs. [12, 13, 5] and characterized by the constant (2.11). In Fig. 2 we show a cross-section of the parameter space by surface $u = 0$, $v = 0$, at which the equation (3.5) turns to the complex analytic map (1.1).

The picture is just a fragment of the Mandelbrot set represented in technique of the Lyapunov chart. The GSK point is located exactly at the center of the diagram. Let us select a small box containing the critical point, enlarge and rotate it in accordance with multiplication by the constant $\delta_1 \cong 4.6002 - 8.9812i$. The resulting diagram is shown at the right part of Fig. 2. In a course of this procedure the legend for the Lyapunov exponent is redefined: as the characteristic time scale of dynamical regimes triplicates, we decrease by 3 times all the values separating the distinct intervals for coding by definite gray tones. Observe excellent visual similarity of both pictures confirming presence of scaling.

Next, let us take another cross-section of the parameter space of the map (3.5), namely, by the surface $a = a_c, b = b_c$. It means that in the parameter space of the original map (3.1) we are on the manifold $M\colon C_1(\lambda, \varepsilon) = 0$. The Lyapunov chart is shown in Fig. 3. Again we have placed the GSK point precisely in the middle of the plot. Observe that visually the picture has nothing common with the familiar Mandelbrot set. However, the self-similarity does hold, although it is linked now with the new scaling constant (2.21). To demonstrate it, let us take a fragment marked by frame, and produce magnification and rotation corresponding to multiplication by $\delta_2 \cong 2.5872 + 1.8067i$. By redefinition of the gray-scale coding rule for the Lyapunov exponent, as on Fig. 2, we obtain the chart presented on the right plot of Fig. 3. It looks remarkably similar to the left diagram, which gives evidence of the expected scaling.

Fig. 4 illustrates how do the Lyapunov charts in the cross-sections $\lambda = \mathrm{const}$ evolve as λ tends

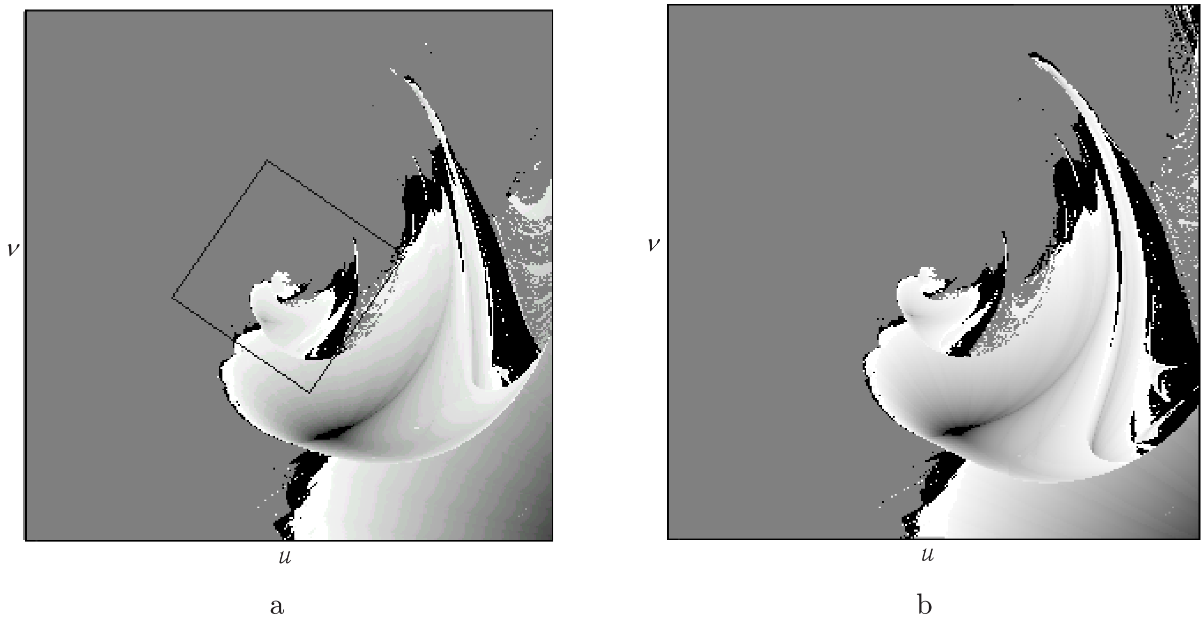

Fig. 3. Cross-section of the parameter space for the map (3.1) by manifold M, on which the perturbation of the RG fixed point associated with senior eigenvalue is excluded. Legend for gray scale coding of the Lyapunov exponent is the same as in Fig. 2. The GSK point is placed exactly at the center of the diagrams. Fig. (b) shows a fragment of Fig. (a) inside the frame after magnification and rotation in accordance with multiplication by δ_2

to the value λ_c associated with the GSK point. The plots are obtained for the cross-sections $\lambda = \lambda_k$, where λ_k correspond to the superstable cycles of period 3^k and are located at the middle of the respective leaves of the Mandelbrot cactus: $\lambda_0 = 0.0+0.0i, \lambda_1 = 0.122561+0.744862i, \lambda_2 = 0.031553+0.790783i, \lambda_3 = 0.023369+0.7846797i$. As we can see, the figure is subsequently enriched by smaller and smaller "bubbles" of decreasing size (shown by arrows). In these domains periodic regimes take place, and the period in each new arising area is tripled in comparison with the previous one. At $\lambda = \lambda_c$ the formation accepts a complete form, which contains an infinite sequence of the bubbles obeying the property of self-similarity. This is the parameter space arrangement on the manifold M. A schema explaining some details of the structure is shown in Fig. 5. The largest area in the middle corresponds to a stable period-1 state. Here the map possesses the fixed point with two (complex conjugate) multipliers, which modulus are less than unity. From the bottom this domain is bounded by a curve, at which the Neimark bifurcation occurs. Here two complex multipliers cross the unit circle. Distinct points of the border differ by the argument of the multipliers at the moment of the bifurcation. For irrational or rational arguments (measured in 2π units) the attractor, which appears as a result of the bifurcation, is, respectively, a torus (in the domain of quasiperiodicity), or a resonance cycle (the Arnold tongues, which are not shown). At the upper border of the stability domain period-doubling bifurcation takes place. It may be followed either by the secondary period doubling (top left part of the border for the period-2 domain), or by Neimark bifurcation (top right part of the border). Note overlap of the period-1 and period-2 areas, which indicates presence of bistability (coexistence of two attractors with distinct basins). In this region the borders of the stability domains are associated with the hard bifurcations (jumps). At the left bottom part of this structure another similarly arranged smaller formation is attached, but there period-3 regime occurs in the middle part of the stability domain. According to results of the RG analysis and scaling arguments, the sequence of the smaller domains, each of which is attached to its precursor, must be infinite and become asymptotically self-similar, accepting a universal form. (In fact, already on the very crude resolution scale of Fig. 5 the domains of periods one and three look remarkably similar.)

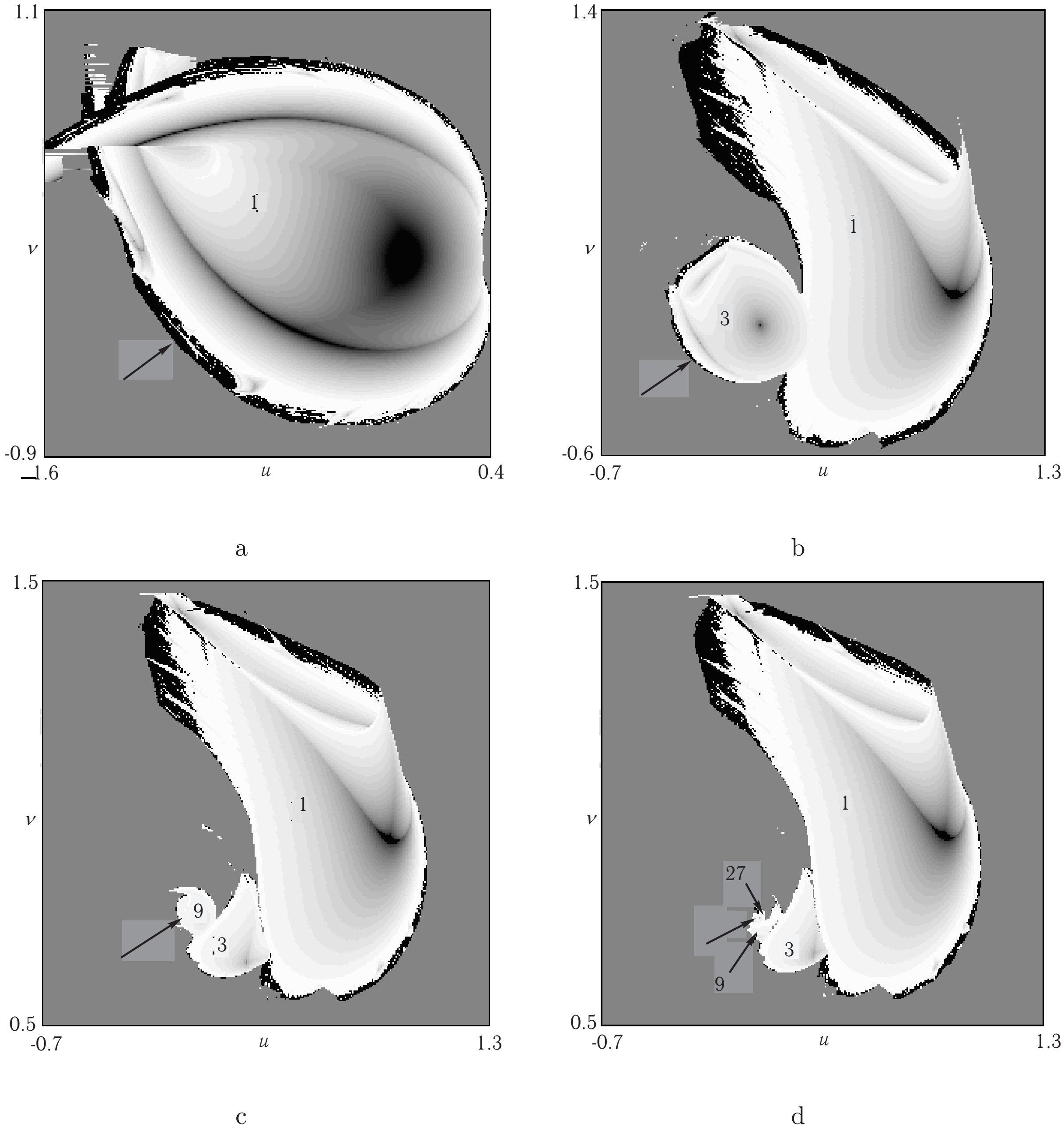

Fig. 4. Lyapunov charts for the map (3.5) on the plane (u, v) obtained at fixed values of λ corresponding at $u = \nu = 0$ to superstable cycles of period 1 (a), 3 (b), 9 (c), 27 (d). Observe that in the cross-sections closer to the GSK point the figure is subsequently enriched by smaller and smaller bubbles (shown by arrows), each new corresponds to the tripled time period

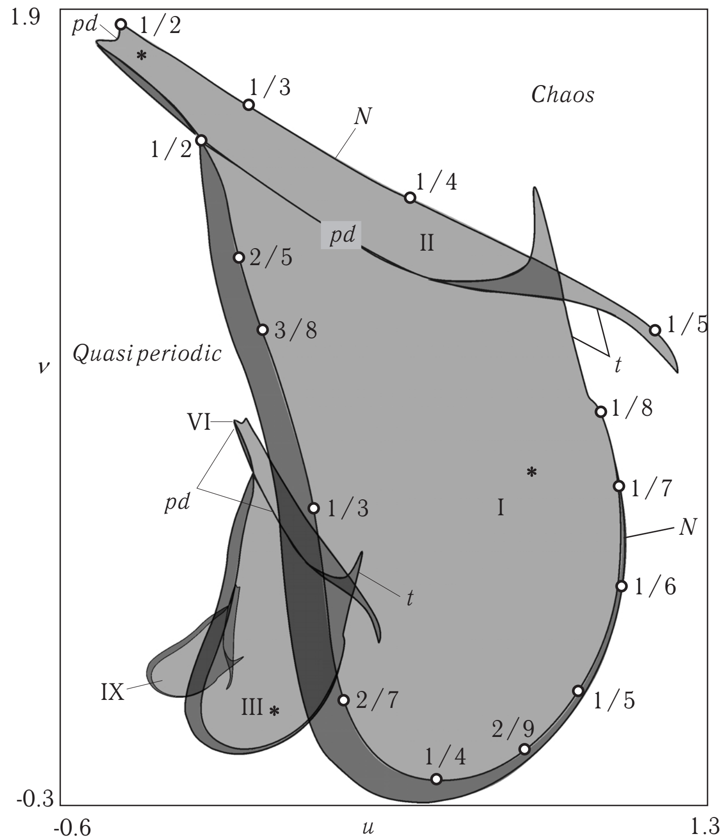

Fig. 5. A schema of the parameter space cross-section by the manifold M, on which the contribution of the senior eigenvector into a perturbation of the RG fixed point is excluded. Light gray areas correspond to periodic regimes of periods marked by the Roman figures. Dark gray designates the area of quasi-periodicity and Arnold tongues. Bifurcation lines are marked as *pd* (period-doubling), *t* (tangent), *N* (Neimark). On the Neimark bifurcation curve some points of rational arguments of the multiplier are marked by circles, these are the sharp ends of the respective Arnold tongues (the tongues themselves are not shown). Figures at that points designate the rotation numbers $\frac{m}{n}$. Stars mark points of existence of superstable cycles

Conclusion

In the present work we have studied scaling properties in the extended parameter space of non-analytic maps for a universality class associated with the period-tripling bifurcation cascade. It is found that the fixed point of the RG equation possesses two relevant eigenvectors, one of which is responsible for the perturbation violating the Cauchy–Riemann conditions. As follows from the RG analysis, the period-tripling universal scaling behavior can occur not only for complex analytic maps; however, in general case, for its observation it is necessary to vanish *two* complex coefficients of the relevant eigenvectors by means of appropriate selection of parameters. In generic case it requires to control at least *four* real parameters. Apparently, experimental observation of such type of behavior in physical systems will be very difficult. Nevertheless, we can not exclude that the period-tripling behaviour can be found in some systems, which possess special symmetries. Perhaps, this is an interesting direction of search for physical applications of the complex analytic dynamics.

This work is supported by RFBR (project No 00-02-17509) and, in part, by Research and Educational Center of Nonlinear Dynamics and Biophysics of Saratov State University via award of US Civilian Research and Development Foundation (CRDF) No REC-006.

Appendix

In Section 3 we have introduced a manifold M in the parameter space of the map (3.1), defined by a condition of absence of the senior eigenvector in the perturbation of the RG fixed point: $C_1(\lambda, \varepsilon) = 0$, or $C_1(a, b; u, v) = 0$. Let us write out the equations for this manifold as

$$a = a_c + F(u, v), \quad F(u, v) = a_c + Au + Bv + Pu^2 + Quv + Rv^2, \tag{4.1}$$
$$b = b_c + G(u, v), \quad G(u, v) = \ b_c + Cu + Dv + Su^2 + Tuv + Hv^2. \tag{4.2}$$

Here, in accordance with the argumentation in the main text, only terms up to the second order in the Taylor expansion are retained. The coefficients designated by the capital letters $A, B, \ldots, H$ have to be computed numerically.

Let us suppose that we have found a cycle of period N for the map (3.1), and this cycle starts at the point (x_0, y_0). In terms of real variables the evolution of small perturbation $(\widetilde{x}, \widetilde{y}) = (\operatorname{Re} \widetilde{z},\ \operatorname{Im} \widetilde{z})$ over one period of the cycle is determined by Jacobi matrix

$$\mathbf{J} = \begin{pmatrix} a_{11} & a_{12} \\ a_{21} & a_{22} \end{pmatrix} = \begin{pmatrix} \dfrac{\partial x_N}{\partial x_0} & \dfrac{\partial x_N}{\partial y_0} \\ \dfrac{\partial y_N}{\partial x_0} & \dfrac{\partial y_N}{\partial y_0} \end{pmatrix}. \tag{4.3}$$

While the map is complex analytic, the Cauchy–Riemann equations hold, namely, $a_{11} = a_{22}$, $a_{12} = -a_{21}$. In presence of the term εz^* these conditions are violated. It is worth considering the trace

$$S = \frac{\partial x_N}{\partial x_0} + \frac{\partial y_N}{\partial y_0} \tag{4.4}$$

and determinant

$$J = \left(\frac{\partial x_N}{\partial x_0}\right)\left(\frac{\partial y_N}{\partial y_0}\right) - \left(\frac{\partial x_N}{\partial y_0}\right)\left(\frac{\partial y_N}{\partial x_0}\right) \tag{4.5}$$

of the matrix $\mathbf{J}$. Note that they are invariant under variable changes. As it has been mentioned (Section 2), exactly at the point GSK an infinite countable set of cycles of period $N = 3, 9, 27, \ldots$, is present. In asymptotics of large k all these cycles have the same universal value of the multipliers, and, hence, are characterized also by the universal values of trace and determinant of the Jacobi matrix.

Let us assume that we have computed the first and the second derivatives of trace and determinant in respect to the parameters u and v for periods 3^{k+1} and 3^k at the point $a = a_c$, $b = b_c$, $u = 0$, $v = 0$. Let us make a small shift of the complex parameter $\varepsilon = u + vi$ from the GSK point, but stay on the manifold M. Then, for the cycle 3^{k+1} the change of the values for trace and determinant should be the same as for the cycle 3^k at the shift $\delta_2\varepsilon = (\xi u - \eta v) + (\xi v + \eta u)i$. The requirement for traces and determinants of both cycles to coincide at arbitrarily chosen u v

$$\begin{aligned} S^{k+1}(u, v) &= S^k(\xi u - \eta v, \xi v + \eta u), \\ J^{k+1}(u, v) &= J^k(\xi u - \eta v, \xi v + \eta u), \end{aligned} \tag{4.6}$$

yields

$$
\begin{aligned}
&S_u^{(k+1)}u + S_v^{(k+1)}v + S_{uv}^{(k+1)}uv + \frac{1}{2}S_{uu}^{(k+1)}u^2 + \frac{1}{2}S_{vv}^{(k+1)}v^2 = \\
&\quad = S_u^{(k)}(\xi u - \eta v) + S_{(v)}^{(k)}(\xi v + \eta u) + S_{uv}^{(k)}(\xi u - \eta v)(\xi v + \eta u) + \\
&\quad + \frac{1}{2}S_{uu}^{(k)}(\xi u - \eta v)^2 + \frac{1}{2}S_{vv}^{(k)}(\xi v + \eta u)^2, \\
&J_u^{(k+1)}u + J_v^{(k+1)}v + J_{uv}^{(k+1)}uv + \frac{1}{2}J_{uu}^{(k+1)}u^2 + \frac{1}{2}J_{vv}^{(k+1)}v^2 = \\
&\quad = J_u^{(k)}(\xi u - \eta v) + J_v^{(k)}(\xi v + \eta u) + J_{uv}^{(k)}(\xi u - \eta v)(\xi v + \eta u) + \\
&\quad + \frac{1}{2}J_{uu}^{(k)}(\xi u - \eta v)^2 + \frac{1}{2}J_{vv}^{(k)}(\xi v + \eta u)^2,
\end{aligned}
\tag{4.7}
$$

where the terms of the first and the second order are accounted.

Equalizing the terms proportional to u and v, we obtain in the first order the following four equations:

$$
\begin{aligned}
S_u^{k+1} &= S_u^k\xi + S_v^k\eta, \quad S_v^{k+1} = S_v^k\xi - S_u^k\eta, \\
J_u^{k+1} &= J_u^k\xi + J_v^k\eta, \quad J_v^{k+1} = J_v^k\xi - J_u^k\eta.
\end{aligned}
\tag{4.8}
$$

for four coefficients A, B, C, D, which influence the first derivatives of trace and determinant. In the second order we equalize the terms proportional to u^2, uv, v^2:

$$
\begin{aligned}
\frac{1}{2}S_{uu}^{k+1} &= \frac{1}{2}S_{uu}^k\xi^2 + S_{uv}^k\xi\eta + \frac{1}{2}S_{vv}^k\eta^2, \\
S_{uv}^{k+1} &= -S_{uu}^k\xi\eta + S_{uv}^k(\xi^2 - \eta^2) + S_{vv}^k\xi\eta, \\
\frac{1}{2}S_{vv}^{k+1} &= \frac{1}{2}S_{uu}^k\eta^2 - S_{uv}^k\xi\eta + \frac{1}{2}S_{vv}^k\xi^2, \\
\frac{1}{2}J_{uu}^{k+1} &= \frac{1}{2}J_{uu}^k\xi^2 + J_{uv}^k\xi\eta + \frac{1}{2}J_{vv}^k\eta^2, \\
J_{uv}^{k+1} &= -J_{uu}^k\xi\eta + J_{uv}^k(\xi^2 - \eta^2) + J_{vv}^k\xi\eta, \\
\frac{1}{2}J_{vv}^{k+1} &= \frac{1}{2}J_{uu}^k\eta^2 - J_{uv}^k\xi\eta + \frac{1}{2}J_{vv}^k\xi^2,
\end{aligned}
\tag{4.9}
$$

and it yields six equations for six unknowns P, Q, R, S, T, U, H.

To obtain the values of the derivatives, we iterate Eqs. (3.5) together with the relations following from them by differentiation in respect to variables and parameters at the point GSK on the periodic orbit under consideration:

$$
\begin{aligned}
x'_x &= -2xx_x + 2yy_x + ux_x + vy_x, \\
y'_x &= -2x_xy - 2xy_x + vx_x - uy_x, \\
x'_u &= -2xx_u + 2yy_u + x + ux_u + vy_u + A + 2Pu + Qv, \\
y'_u &= -2x_uy - 2xy_u + vx_u - y - uy_u + C + 2Su + Tv, \\
x'_v &= -2xx_v + 2yy_v + ux_v + vy_v + y + B + Qu + 2Rv, \\
y'_v &= -2x_vy - 2xy_v + vx_v - uy_v + x + D + Tu + 2Hv,
\end{aligned}
\tag{4.10}
$$

$$
\begin{aligned}
x'_{uu} &= -2x_ux_u - 2xx_{uu} + 2y_uy_u + 2y_{uu} + x_u + ux_{uu} + vy_{uu} + 2P, \\
x'_{uv} &= -2x_ux_v - 2xx_{uv} + 2y_uy_v + 2y_{uv} + x_v + ux_{uv} + y_u + vy_{uv} + Q, \\
x'_{vv} &= -2x_vx_v - 2xx_{vv} + 2y_vy_v + 2y_{vv} + y_v + ux_{vv} + vy_{vv} + 2R, \\
y'_{uu} &= -2x_{uu}y - 2x_uy_u - 2x_uy_u - 2xy_{uu} + vx_{uu} - y_u - uy_{uu} + 2S, \\
y'_{uv} &= -2x_{uv}y - 2x_uy_v - 2x_vy_u - 2xy_{uv} + x_u + vx_{uv} - y_v - uy_{uv} + T, \\
y'_{vv} &= -2x_{vv}y - 2x_vy_v - 2x_vy_v - 2xy_{vv} + x_v + vx_{vv} - uy_{vv} + 2H,
\end{aligned}
\tag{4.11}
$$

$$
\begin{aligned}
x'_{xu} &= -2x_u x_x - 2x x_{xu} + 2y_u y_x + 2y_{xu} + x_x + u x_{xu} + v y_{xu},\\
y'_{xu} &= -2x_{xu} y - 2x_x y_u - 2x_u y_x - 2x y_{xu} + v x_{xu} - y_x - u y_{xu},\\
x'_{xv} &= -2x_v x_x - 2x x_{xv} + 2y_v y_x + 2y_{xv} + u x_{xv} + y_x + v y_{xv},\\
y'_{xv} &= -2x_{xv} y - 2x_x y_v - 2x_v y_x - 2x y_{xv} + x_x + v x_{xv} - u y_{xv},\\
x'_{yu} &= -2x_u x_y - 2x x_{yu} + 2y_u y_y + 2y_{yu} + x_y + u x_{yu} + v y_{yu},\\
y'_{yu} &= -2x_{yu} y - 2x_y y_u - 2x_u y_y - 2x y_{yu} + v x_{yu} - y_y - u y_{yu},\\
x'_{yv} &= -2x_v x_y - 2x x_{yv} + 2y_v y_y + 2y_{yv} + u x_{yv} + y_y + v y_{yv},\\
y'_{yv} &= -2x_{yv} y - 2x_y y_v - 2x_v y_y - 2x y_{yv} + x_y + v x_{yv} - u y_{yv},
\end{aligned}
\tag{4.12}
$$

$$
\begin{aligned}
x'_{xuu} &= -2x_{uu}x_x - 4x_u x_{xu} - 2x x_{xuu} + 2y_{uu} y_x + 4y_u y_{xu} + 2y y_{xuu} + 2x_{xu} + u x_{xuu} + v y_{xuu},\\
x'_{xuv} &= -2x_{uv}x_x - 2x_v x_{xu} - 2x_u x_{xv} - 2x x_{xuv} + 2y_{uv} y_x + 2y_v y_{xu} + 2y_u y_{xv} + 2y y_{xuv} +\\
&\quad + x_{xv} + u x_{xuv} + y_{ux} + v y_{xuv},\\
x'_{xvv} &= -2x_{vv}x_x - 4x_v x_{xv} - 2x x_{xvv} + 2y_{vv} y_x + 4y_v y_{xv} + 2y y_{xvv} + 2y_{xv} + u x_{xvv} + v y_{xvv},\\
y'_{xuu} &= -2x_{xuu} y - 4x_{xu} y_u - 2x_x y_{uu} - 2x_{uu} y_x - 4x_u y_{xu} - 2x y_{xuu} - 2y_{xu} + v x_{xuu} - u y_{xuu},\\
y'_{xuv} &= -2x_{xuv} y - 2x_{xv} y_u - 2x_{xu} y_v - 2x_x y_{uv} - 2x_{uv} y_x - 2x_v y_{xu} - 2x_u y_{xv} - 2x y_{xuv} +\\
&\quad + 2x_{xu} + v x_{xuv} - y + xv - u y_{xuv},\\
y'_{xvv} &= -2x_{xvv} y - 4x_{xv} y_v - 2x_x y_{vv} - 2x_{vv} y_x - 4x_v y_{xv} - 2x y_{xvv} + x_x v + x_{xv} + v x_{xvv} - u y_{xvv},\\
x'_{yuu} &= -2x_{uu}x_y - 4x_u x_{yu} - 2x x_{yuu} + 2y_{uu} y_y + 4y_u y_{yu} + 2y y_{yuu} + 2x_{yu} + u x_{yuu} + v y_{yuu},\\
x'_{yuv} &= -2x_{uv}x_y - 2x_v x_{yu} - 2x_u x_{yv} - 2x x_{yuv} + 2y_{uv} y_y + 2y_v y_{yu} + 2y_u y_{yv} + 2y y_{yuv} +\\
&\quad + x_{yv} + u x_{yuv} + y_{uy} + v y_{yuv},\\
x'_{yvv} &= -2x_{vv}x_y - 4x_v x_{yv} - 2x x_{yvv} + 2y_{vv} y_y + 4y_v y_{yv} + 2y y_{yvv} + 2y_{yv} + u x_{yvv} + v y_{yvv},\\
y'_{yuu} &= -2x_{yuu} y - 4x_{yu} y_u - 2x_y y_{uu} - 2x_{uu} y_y - 4x_u y_{yu} - 2x y_{yuu} - 2y_{yu} + v x_{yuu} - u y_{yuu},\\
y'_{yuv} &= -2x_{yuv} y - 2x_{yv} y_u - 2x_{yu} y_v - 2x_y y_{uv} - 2x_{uv} y_y - 2x_v y_{yu} - 2x_u y_{yv} - 2x y_{yuv} +\\
&\quad + 2x_{yu} + v x_{yuv} - y + yv - u y_{yuv},\\
y'_{yvv} &= -2x_{yvv} y - 4x_{yv} y_v - 2x_y y_{vv} - 2x_{vv} y_y - 4x_v y_{yv} - 2x y_{yvv} + x_y v + x_{yv} + v x_{yvv} - u y_{yvv},
\end{aligned}
\tag{4.13}
$$

Initial conditions for all iterated variables are formulated as follows:

$$
\begin{gathered}
x = x_0, \quad y = y_0,\\
x_u = x_{u0}, \quad y_u = y_{u0}, \quad x_v = x_{v0}, \quad y_v = y_{v0},\\
x_{uu} = x_{uu0}, y_{uu} = y_{uu0}, x_{uv} = x_{uv0}, y_{uv} = y_{uv0}, x_{vv} = x_{vv0}, y_{vv} = y_{vv0},\\
x_x = 1, \quad x_y = 0, \quad y_x = 0, \quad y_y = 1,\\
x_{xu} = x_{yu} = x_{xv} = x_{yv} = y_{xu} = y_{yu} = y_{xv} = y_{yv} = 0,\\
x_{xuu} = x_{xuv} = x_{xvv} = x_{yuu} = x_{yuv} = x_{yvv} = 0,\\
y_{xuu} = y_{xuv} = y_{xvv} = y_{yuu} = y_{yuv} = y_{yvv} = 0.
\end{gathered}
\tag{4.14}
$$

Constants x_0, y_0, x_{u0}, y_{u0}, x_{v0}, y_{v0}, x_{uu0}, y_{uu0}, x_{uv0}, y_{uv0}, x_{vv0}, y_{vv0} are determined in a process of the calculations with Newton method to satisfy the condition that the values of the respective variables after a period of the cycle have to be equal to their initial values.

Trace and determinant of the Jacobi matrix and their derivatives are defined as

$$
\begin{gathered}
S = x_x + y_y, \\
S_u = x_{xu} + y_{yu}, \quad S_v = x_{xv} + y_{yv}, \\
S_{uu} = x_{xuu} + y_{yuu}, S_{uv} = x_{xuv} + y_{yuv}, S_{vv} = x_{xvv} + y_{yvv}, \\
J = x_x y_y - x_y y_x, \\
J_u = x_{xu} y_y + x_x y_{yu} - x_{yu} y_x - x_y y_{xu}, \quad J_v = x_{xv} y_y + x_x y_{yv} - x_{yv} y_x - x_y y_{xv}, \\
J_{uu} = x_{xuu} y_y + x_{xu} y_{yu} + x_{xu} y_{yu} + x_x y_{yuu} - x_{yuu} y_x - x_{yu} y_{xu} - x_{yu} y_{xu} - x_y y_{xuu}, \\
J_{uv} = x_{xuv} y_y + x_{xu} y_{yv} + x_{xv} y_{yu} + x_x y_{yuv} - x_{yuv} y_x - x_{yu} y_{xv} - x_{yv} y_{xu} - x_y y_{xuv}, \\
J_{vv} = x_{xvv} y_y + x_{xv} y_{yv} + x_{xv} y_{yv} + x_x y_{yvv} - x_{yvv} y_x - x_{yvv} y_{xv} - x_y y_{xvv},
\end{gathered} \tag{4.15}
$$

The final result of the computation is given by the numerical data for the coefficients (3.6).

References

[1] *H.-O. Peitgen, P. H. Richter.* The Beauty of Fractals. Images of Complex Dynamical Systems. Springer-Verlag, 1986.

[2] *R. L. Devaney.* An Introduction to Chaotic Dynamical Systems. Addison-Wesley Publ, 1989.

[3] *K. M. Briggs, G. R. W. Quispel, C. J. Tomphson.* Feigenvalues for Mandelsets. J. Phys. A24, No 14, 1991, P. 3363–3368.

[4] *J. Milnor.* Self-Similarity and Hairiness in the Mandelbrot Set. Computers in Geometry and Topology, 114, 1989, P. 211–257.

[5] *P. Cvitanović, J. Myrheim.* Complex Universality. Commun. Math. Phys., 121, No 2, 1989, P. 225–254.

[6] *M. J. Feigenbaum.* Quantitative Universality for a Class of Non-Linear Transformations. J. Stat. Phys., 19, No 1, 1978, P. 25–52.

[7] *M. J. Feigenbaum.* The Universal Metric Properties of Non-Linear Transformations. J. Stat. Phys., 21, No 6, 1979, P. 669–706.

[8] *M. Feigenbaum.* Universality in Behavior of Nonlinear Systems. Usp. Fiz. Nauk, V. 141, No 2, 1983, P. 343–374.

[9] *E. B. Vul, Y. G. Sinai, K. M. Khanin.* Feigenbaum Universality and the Thermodynamic Formalism. Russ. Math. Surv., 39, No 3, 1984, P. 1–40.

[10] *M. Nauenberg.* Fractal Boundary of Domain of Analyticity of the Feigenbaum Function and Relation to the Mandelbrot Set. J. Stat. Phys., V. 47, No 3–4, 1987, P. 459–475.

[11] *A. L. J. Wells, R. E. Overill.* The Extension of the Feigenbaum – Cvitanović Function to the Complex Plane. Int. J. of Bifurcation and Chaos. V. 4, No 4, 1994, P. 1041–1051.

[12] *A. I. Golberg, Y. G. Sinai, K. M. Khanin.* Universal Properties for Sequences of Bifurcations of Period 3. Russ. Math. Surv., V. 38, No 1, 1983, P. 187–188.

[13] *P. Cvitanović, J. Myrheim.* Universality for Period n-Tuplings in Complex Mappings. Phys. Lett. A94, No 8, 1983, P. 329–333.

[14] *C. Beck.* Physical Meaning for Mandelbrot and Julia Set. Physica D125, 1999, P. 171–182.

[15] *G. H. Gunaratne.* Trajectory Scaling for Period Tripling in Near Conformal Mappings. Phys. Rev. A36, 1987, P. 1834–1839.

[16] *J. Peinke, J. Parisi, B. Rohricht, O. E. Rossler.* Instability of the Mandelbrot Set. Zeitsch. Naturforsch. A42, No 3, 1987. P. 263–266.

[17] *M. Klein.* Mandelbrot Set in a Non-Analytic Map. Zeitsch. Naturforsch. A43, No 8–9, 1988, P. 819–820.

[18] *B. B. Peckham.* Real Perturbation of Complex Analytic Families: Points to Regions. Int. J. of Bifurcation and Chaos, V. 8, No 1, 1998, P. 73–93.

[19] *B. B. Peckham, J. Montaldi.* Real Continuation from the Complex Quadratic Family: Fixed-Point Bifurcation Sets. Int. J. of Bifurcation and Chaos, V. 10, No 2, 2000, P. 391–414.

[20] *J. Argyris, I. Andreadis, T. E. Karakasidis.* On Perturbations of the Maldelbrot Map. Chaos, Solitons & Fractals, V. 11, No 7, 2000, P. 1131–1136.

[21] *J. Rössler, M. Kiwi, B. Hess, M. Marcus.* On Perturbations Modulated Non-Linear Processes and a Novel Mechanism to Induce Chaos. Phys. Rev. A39, No 11, 1989, P. 5954–5960.

[22] *M. Marcus, B. Hess.* Lyapunov Exponents of the Logistic Map with Periodic Forcing. Computers & Graphics, V. 13, No 4, 1989, P. 553–558.

[23] *J. C. Bastos de Figueiredo, C. P. Malta.* Lyapunov Graph for Two-Parameters Map: Application to the Circle Map. Int. J. of Bifurcation and Chaos, V. 8, No 2, 1998, P. 281–293.

[24] *A. P. Kuznetsov, S. P. Kuznetsov, I. R. Sataev.* Three-Parameter Scaling for One-Dimensional Maps. Phys. Lett. A189, No 5, 1994, P. 367–373.

[25] *A. P. Kuznetsov, S. P. Kuznetsov, I. R. Sataev.* A Variety of the Period-Doubling Universality Classes in Multi-Parameter Analysis of Transition to Chaos. Physica D109, No 1–2, 1997, P. 91–112.

[26] *S. P. Kuznetsov, E. Neumann, A. Pikovsky, I. R. Sataev.* Critical Point of Tori Collision in Quasiperiodically Forced Systems. Phys. Rev. E62, No 2, 2000, P. 1995–2007.